RSC Advances

PAPER

View Article Online
View Journal | View Issue

Cite this: *RSC Adv.*, 2023, **13**, 17051

Magnetite-supported montmorillonite (K_{10}) (nanocat-Fe-Si-K_{10}): an efficient green catalyst for multicomponent synthesis of amidoalkyl naphthol†

Shripad M. Patil, [ab] Runjhun Tandon, *[a] Nitin Tandon,[a] Iqubal Singh,[a] Ashwini Bedre[b] and Vilas Gade[c]

Received 8th March 2023
Accepted 18th May 2023

DOI: 10.1039/d3ra01522j

rsc.li/rsc-advances

Montmorillonite (K_{10}) loaded on magnetite silica-coated nanoparticles was made using simple co-precipitation methods. The prepared nanocat-Fe-Si-K_{10} was analyzed using some techniques including field emission-scanning electron microscopy (FE-SEM), inductive coupling plasma-optical emission spectroscopy (ICP-OES), X-ray diffraction (XRD), thermo-gravimetric analysis (TGA), Fourier transmission-infrared spectra (FT-IR), energy dispersive X-ray spectroscopy (EDS), and wavelength-dispersive spectroscopy (WDX). The catalytic activity of the synthesized nanocat-Fe-Si-K_{10} has been examined in one-pot multicomponent transformations for the synthesis of 1-amidoalkyl 2-naphthol derivatives under solvent-free conditions. Nanocat-Fe-Si-K_{10} was determined to be very active, having the ability to be reused 15 times without significant loss of catalytic activity. The suggested technique has several advantages, including excellent yield, minimum reaction time, a straightforward workup, and catalyst recycling, all of which are essential green synthetic aspects.

1 Introduction

Among the most critical and essential C–C bond forming processes in chemical synthesis is indeed the Betti reaction, this is a kind of Mannich type reaction.[1] The Betti reaction provides 1-(α-amino-alkyl)-2-naphthol, the so-called Betti bases. Betti bases are valuable ligands in synthetic chemistry.[2,3] Betti bases are becoming increasingly prominent in medicine because of their biologically active compounds,[52,55] which exhibit properties including anti-pain, antibacterial, and antihypertensive properties.[4–6]

As in the presence of an aldehyde, urea, or ammonia, α-naphthol interacts with sodium hydroxide in two steps over a long period.[7] The chemically produced approach, on the other hand, has several significant flaws and is limited in its use. As a result, numerous different forms of the Betti response have been developed to solve the flaws in the classic technique. In particular, a multi-component technique that replaces ammonia with naphthol, alkyl amines, and quinols is recommended since it allows for a wide range of possible alterations.[8–10] On the other hand, these treatments were marred by considerable side effects, longer reaction times, and reduced output. In terms of the green approach, multi-component reactions under aqueous conditions are beneficial because they provide easy and quick access to a large variety of organic molecules.[7,11]

The Betti reaction is difficult to deal with in water because the reactivity of amine is primarily constrained by strong hydrogen bonding. Sulfanilic acid-functionalized silica-decorated ferrite nanoparticles,[12] triflate,[13] and imidazolium compounds,[14,15] all unique metal and transition elements,[16] have all been successfully employed as Mannich processes in aqueous or without solvent.[17,18] The catalysts were neither inaccessible nor recyclable in the vast majority of reactions. Because of its electron-withdrawing group and steric crowded, amines substrate are still a problem to use as derivatives in aqueous to our awareness. As a result, ecologically and green

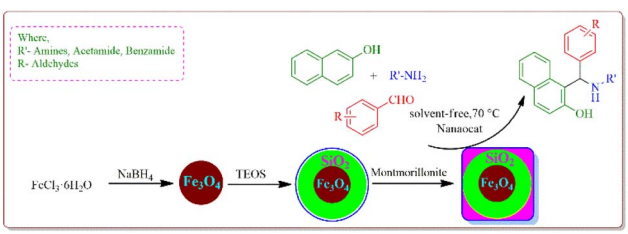

Scheme 1 Synthesis of Fe_3O_4@SiO_2@K_{10} nanoparticles applicable in multicomponent reaction.

[a]School of Chemical Engineering and Physical Science, Lovely Professional University, Phagwara-144411, Punjab, India. E-mail: patilshripad55@gmail.com; runjhun.19532@lpu.co.in

[b]Savitribai Phule Pune University, Dada Patil Mahavidyalaya, Karjat-414401, Maharashtra, India

[c]Rayat Shikshan Sanstha's, Arts, Science & Commerce College, Mokhada, Palghar-401604, Maharashtra, India

† Electronic supplementary information (ESI) available. See DOI: https://doi.org/10.1039/d3ra01522j

catalysis approaches are necessary for reactions like the Betti reaction. A multicomponent reaction under aromatic aldehydes, amide, and α-naphthol was carried out in the presence of various Brønsted or Lewis acid catalysts to obtain 1-amidoalkyl 2-naphthols. A range of physiologically significant organic ingredients, oligonucleotide antibiotics, HIV protease, and other chemicals possess 1,3-amino reactive hydroxyl units.[19–21] The amide hydrolysis process can transform 1-amidoalkyl 2-naphthols to beneficial and biological functions construction materials as well as amido methyl naphthols, which have depressant effects and hypotension.[22] A few of the catalysts used in the production of 1-amidoalkyl 2-naphthols have been described including that $Ce(SO_4)_2$,[23] iodine,[24] $K_5CoW_{12}O_{40}\cdot 3H_2O$,[25] montmorillonite K_{10} clay,[26] dodecylphosphonic acid,[27] $H_4SiW_{12}O_{40}$,[28] $HClO_4$–SiO_2,[29] and $Fe(HSO_4)_3$ (ref. 30) *etc.* Unfortunately, several of the approaches mentioned in this article have drawbacks, which including toxic solvents, slow reaction times, a costly reagent, a poor yield, and unpleasant chemical modification like elevated temperature are all factors to consider.[47–50] Due to the limitations of prior approaches, it is critical to creating environmentally-friendly cleaner techniques with strong catalytic performance for the synthesis of 1-amidoalkyl-2-naphthols to achieve sustainable development. Furthermore, from the aspect of environmental remediation, the absence of solvent techniques to biochemical processes is a rising tendency in respect of potential materials and harmful by-products.[31]

We used a straightforward approach to make Fe_3O_4@-SiO_2@K_{10} nanoparticles in this investigation. The first stage included using a straightforward co-precipitation process to make ferrite nanoparticles. The ferrite nanoparticles were coated with silica and tetraethyl orthosilicate (TEOS) using the Stober method. Subsequently, montmorillonite (K_{10}) was used to make K_{10}-supported silica-decorated nanoparticles (Fe_3O_4@SiO_2@K_{10}). The 1-amidoalkyl 2-naphthols were prepared under solvent-free conditions using this Fe_3O_4@SiO_2@K_{10} nanoparticle (Scheme 1).

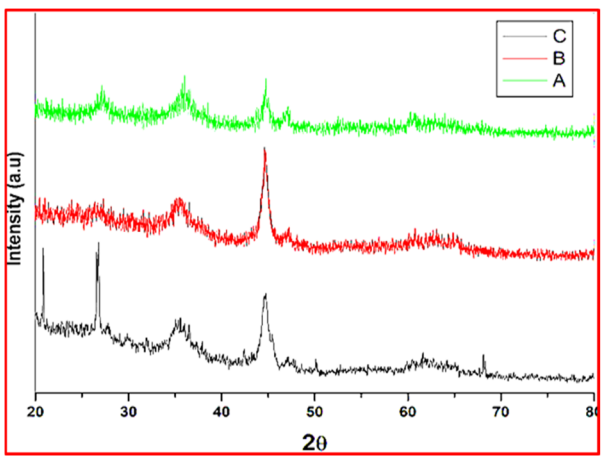

Fig. 1 Powder XRD peak of (A) ferrite (B) silica-coated ferrite (C) K_{10} functionalized silica-coated ferrite nanoparticles.

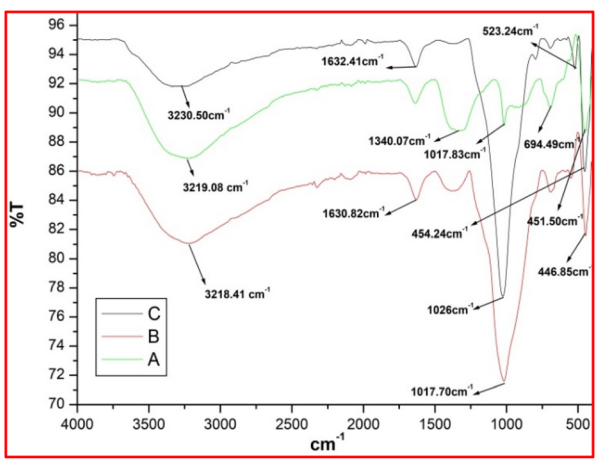

Fig. 2 FT-IR spectra of (A) ferrite (B) silica-coated ferrite (C) K_{10} functionalized silica-coated ferrite nanoparticles.

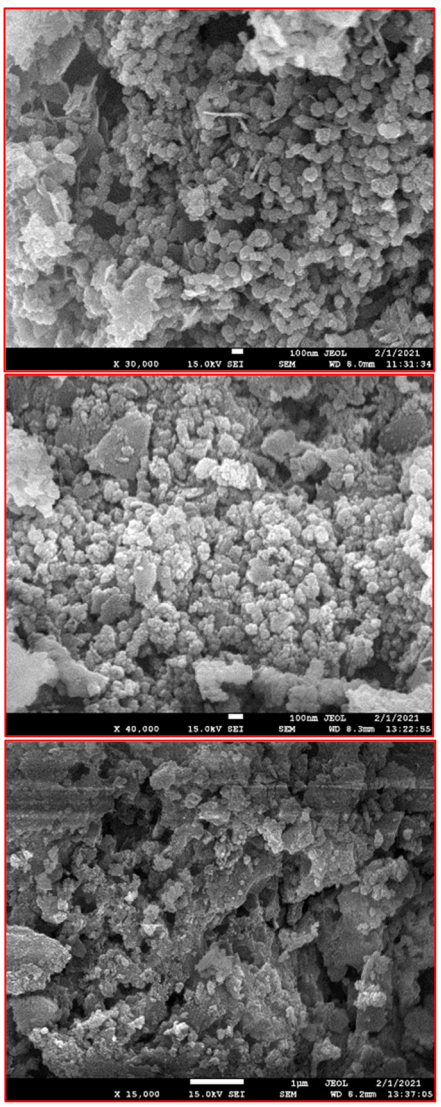

Fig. 3 SEM images of (A) ferrite (B) silica-coated ferrite (C) K_{10}-supported silica-ferrite nanoparticle.

2 Results and discussion

2.1 Characterization of the prepared nanocatalyst

Montmorillonite (K_{10}) functionalized magnetic nanoparticles were studied using XRD, FT-IR, EDS, and FE-SEM, TGA, TEM and ICP-OES analysis methods. XRD methods were used to investigate the morphology of montmorillonite K_{10}-supported silica-coating nanocrystals. All the characterized data are similar to the previously reported work.[51]

Fig. 1 the synthesized nanocatalyst was studied using a powder XRD pattern between 20° and 80°. The iron nanoparticles were encapsulated with tetraethyl orthosilicate (TEOS), resulting in a reduced diffraction pattern. The diffraction pattern of the produced nanostructures is unaffected. By using the Scherrer equation and the full-width at half maximum of a larger signal of XRD pattern, the particles size was determined to be 19 nm (26.5).[51] Because of the low content of K_{10}, the peak is not evident in PXRD spectra. The peak for Al, Mg, and K was not observed in the powder XRD pattern, probably due to the low amount of elements being (about 0.57, 0.35, and 0.11 total amount of montmorillonite-1.03% by ICP-OES analysis).

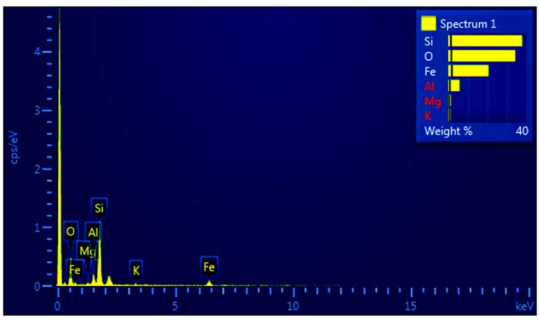

Fig. 4 EDX profile of K_{10} supported silica-ferrite nanoparticles.

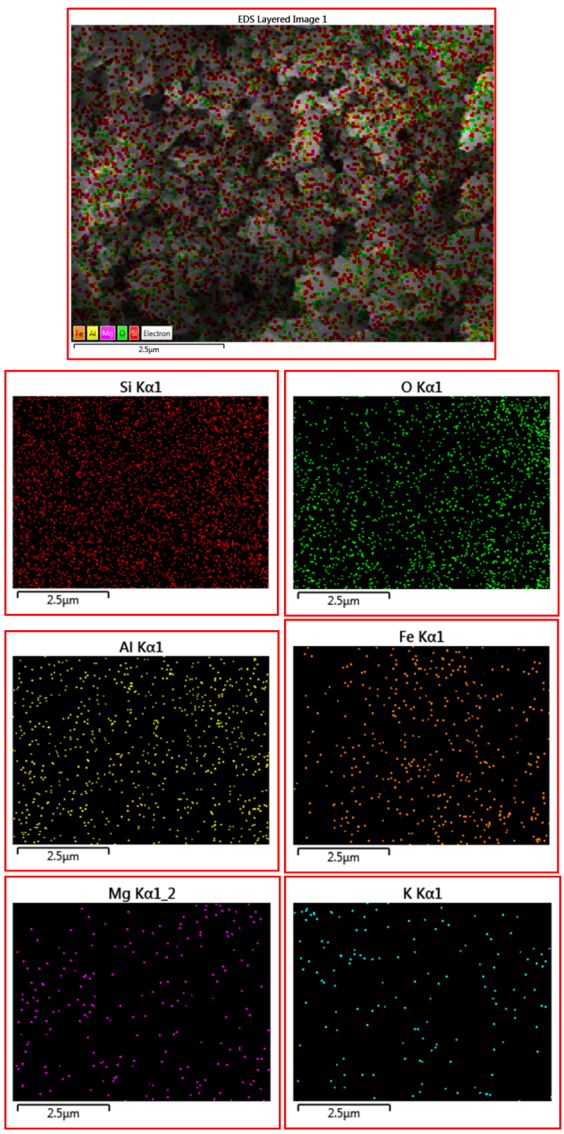

Fig. 5 SEM images of K_{10} functionalized silica-ferrite nanoparticles seen in the presence of Si, O, Al, Fe, Mg, and K atom.

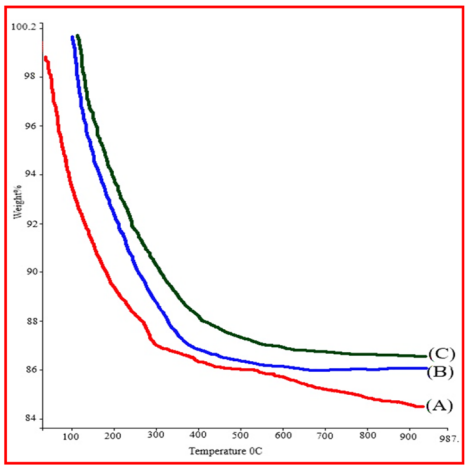

Fig. 6 Thermo-gravimetric analysis of (A) Fe_3O_4, (B) Fe_3O_4@SiO_2, (C) Fe_3O_4@SiO_2@K_{10} nanocatalysts.

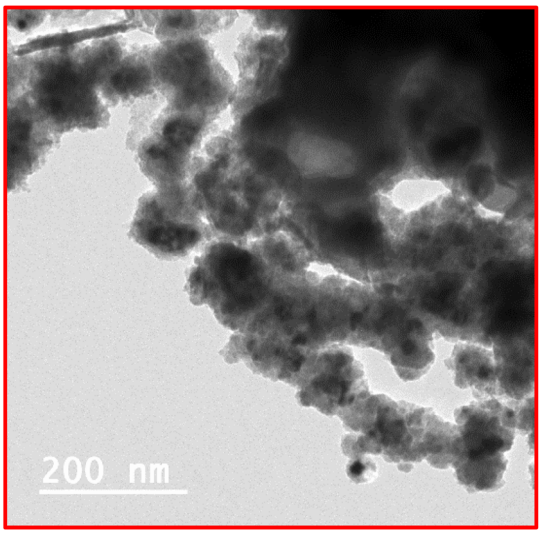

Fig. 7 TEM image of the Fe_3O_4@SiO_2@K_{10} nanocatalyst.

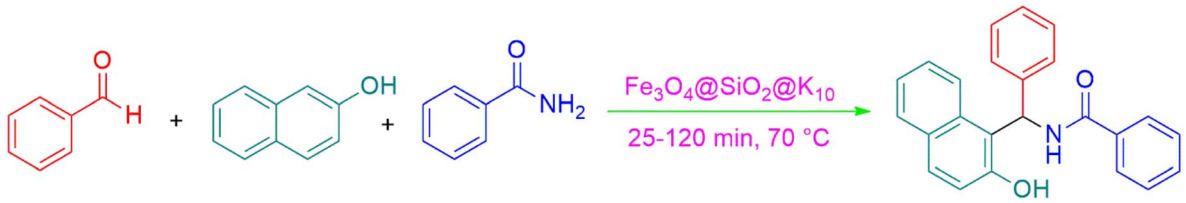

Scheme 2 Reaction of β-naphthol, benzaldehyde and benzamide catalyzed by Fe_3O_4@SiO_2@Montmorillonite nanocatalyst.

In this paper, the spectra of magnetite nanoparticles in the infrared range are discussed Fig. 2A.[53,54] The significant signal at 3219.08 cm^{-1} indicates the OH stretching bandwidth of the molecule of water depicted in the sample. The signal has found at 1340.07 cm^{-1} and 1017.83 cm^{-1}, which indicated the presence of deionized water. The peaks 451.50 cm^{-1} and 694.49 cm^{-1} were emerge so at O–Fe bonding vibration. Two characteristic peaks inside the IR spectra of silica ferrite nanocrystals, at 1630.82 cm^{-1} and 1017.70 cm^{-1}, suggest symmetrical and unsymmetrical stretching frequencies of the silica–oxygen–silica bond, correspondingly. Fig. 2B the bending resonance frequency of Si–O–Si is 446.85 cm^{-1}. Ir spectrum of K_{10} mediated silica ferrite nanoparticles Fig. 2C, which provides at 523.24 cm^{-1} maxima, the Al–O–Si connection is visible. Another peak appears at 451.50 cm^{-1}, indicating the wavelength of Si–O–Si bending vibrations.[51]

Table 1 Optimization of different reaction condition for the preparation of amidoalkyl naphthol[a]

Sr. no.	Solvent	Catalyst (mg)	Temp. (°C)	Time (min)	Yield[b] (%)
1	None	None	90 °C	2 h	NR[c]
2	None	0.07	90 °C	40 min	85
3	None	0.07	70 °C	40 min	79
4	None	0.07	60 °C	40 min	65
5	None	0.08	70 °C	25 min	96
6	None	0.09	70 °C	25 min	96
7	CH_3CN	0.08	Reflux	2 h	55
8	THF	0.08	Reflux	2 h	53
9	EtOH	0.08	Reflux	2 h	45
10	MeOH	0.08	Reflux	2 h	50
11	Toluene	0.08	Reflux	2 h	47
12	DCM	0.08	Reflux	2 h	40

[a] Reaction condition: β-naphthol (10 mmol), benzaldehyde (10 mmol), and benzamide (12 mmol) solvent-free or solvent (5 mL). [b] Isolated product. [c] No reaction.

The study under Scanning Electron Microscope (SEM) pictures of ferrite, silica ferrite, and K_{10} functionalized silica ferrite nanoparticles are shown in (Fig. 3A–C). In a Scanning electron microscope (SEM) the K_{10} functionalized silica ferrite nanoparticle appears to be spherical. The prepared ferrite, silica-ferrite, and K10-supported silica-ferrite nanoparticles showed 78, 88, and 96 nm particle sizes. The EDX analysis has been used in combination with SEM to examine K_{10} functionalized silica ferrite nanoparticles, revealing O, Fe, Si, Al, Mg, and K as shown in Fig. 4.

This study was examined SEM (scanning electron microscopy) with WDX (wavelength dispersive X-ray spectra). This resulted in the primary analysis of the data of various chemical constituents in nanocrystals. The O, Mg, Al, K, Si, and Fe atoms were observed in the ratios of 39.9, 1.15, 5.56, 37.74, 0.93, and 20.93 percent, respectively in the EDX spectrum of K_{10} decorated silica-ferrite nanoparticles present in the homogeneous states Fig. 5.

The TGA (thermo-gravimetric analysis) was investigated for Fe_3O_4, Fe_3O_4@SiO_2, and Fe_3O_4@SiO_2@K_{10} nanocatalyst at 30 °C to 1000 °C in air atmosphere as shown in Fig. 6. In the (Fig. 6A and B) TGA (thermo-gravimetric analysis) of Fe_3O_4@SiO_2 and Fe_3O_4 nanoparticles indicated a slight weight loss below 200 °C, which was ascribed to the loss of adsorbed water in this study. The TGA (thermo-gravimetric analysis) curve of Fe_3O_4@SiO_2@K_{10} shows significant weight loss at 200 °C, with additional weight loss occurring above 400–600 °C due to the breaking of montmorillonite K_{10} (Fig. 6C).

The relevant pictures are exhibited in Fig. 7 and were obtained through the use of TEM analysis to learn more about the specific surface area of nanoparticles made Fe_3O_4@SiO_2@K_{10}. After the formation of Fe_3O_4@SiO_2@K_{10} nanoparticle was observed as ferrite showed black dots and silica-coating on the ferrite surface. Fe_3O_4@SiO_2@K_{10} nanoparticles were found to be evenly dispersed and have a diameter of around 200 nm.

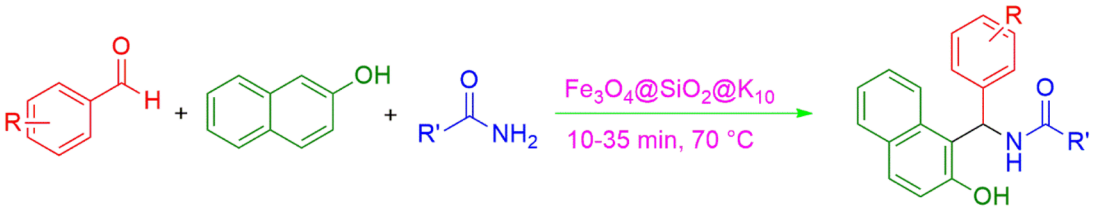

Scheme 3 Scope of the substrate for the synthesis of amidoalkyl naphthol derivatives.

Table 2 Synthesis of amidoalkyl naphthol under solvent-free catalyzed by $Fe_3O_4@SiO_2@K_{10}$[a]

Sr. no.	Aldehyde (R)	Naphthol	Amide (R′)	Product	Time (min)	Yield[b] (%)
1	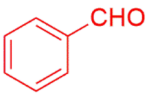	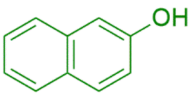	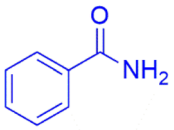	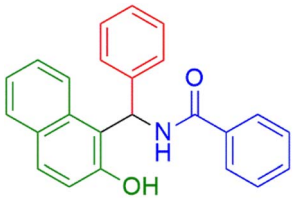	25	96
2	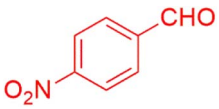	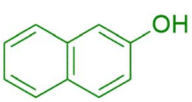	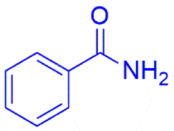	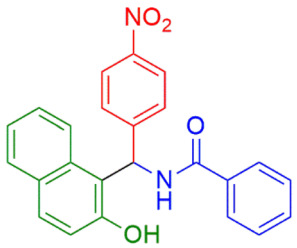	20	98
3	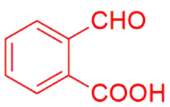	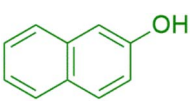	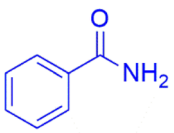	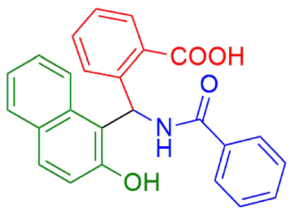	20	94
4	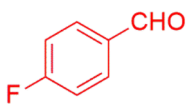	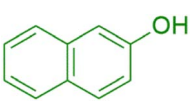	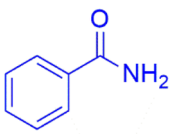	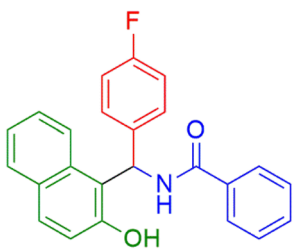	25	95
5	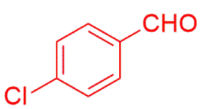	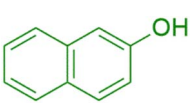	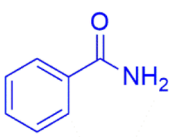	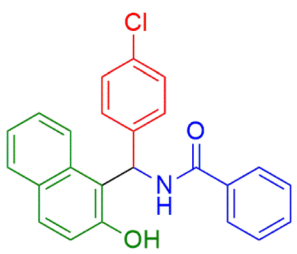	30	90
6	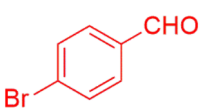	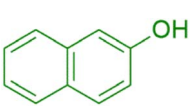	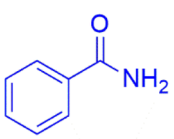	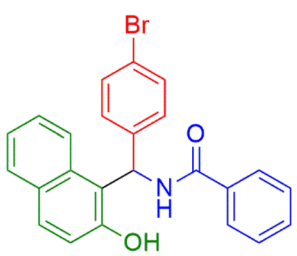	25	91

Table 2 (*Contd.*)

Sr. no.	Aldehyde (R)	Naphthol	Amide (R′)	Product	Time (min)	Yield[b] (%)
7	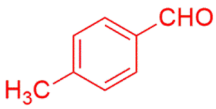	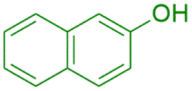	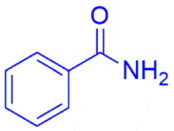	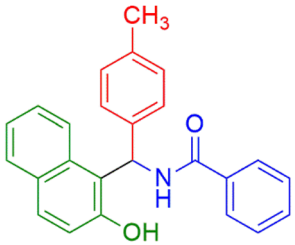	20	94
8	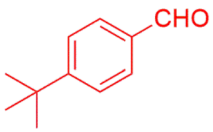	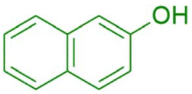	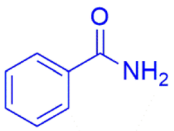	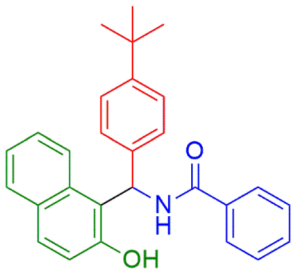	15	96
9	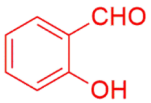	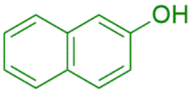	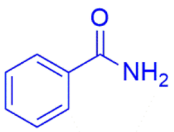	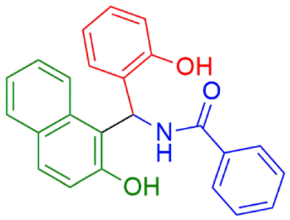	30	88
10	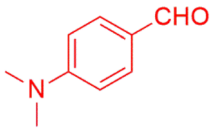	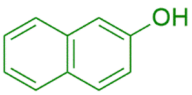	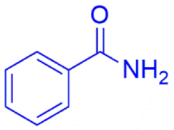	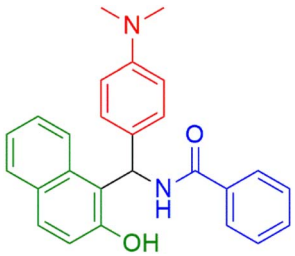	35	90
11		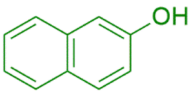	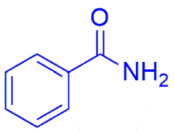	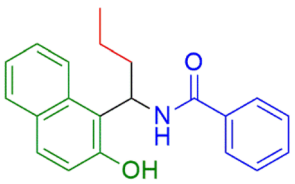	10	96
12	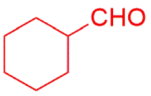	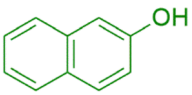	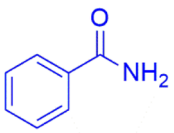	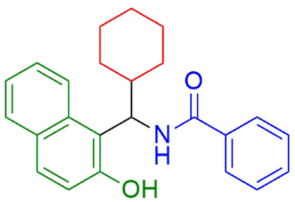	15	95
13	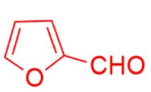	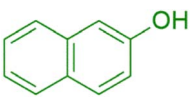	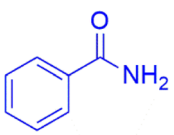	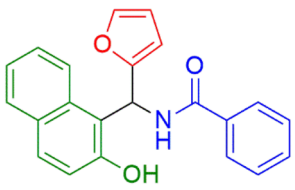	15	96

Table 2 (*Contd.*)

Sr. no.	Aldehyde (R)	Naphthol	Amide (R′)	Product	Time (min)	Yield[b] (%)
14	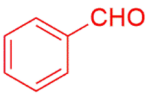	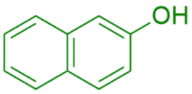	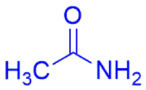	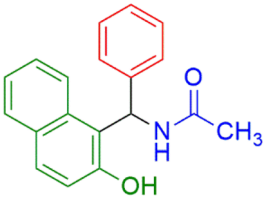	10	97
15	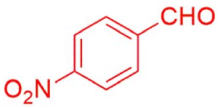	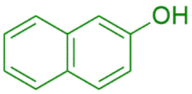	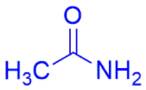	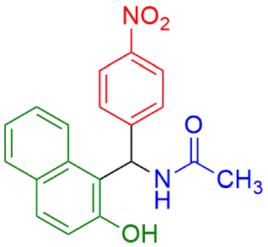	15	97
16	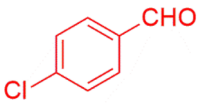	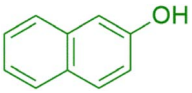	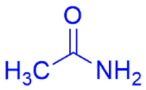	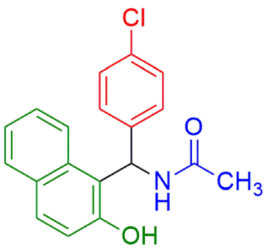	15	97
17	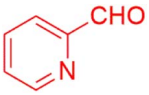	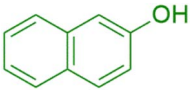	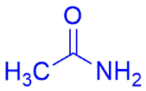	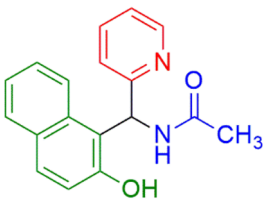	10	96
18	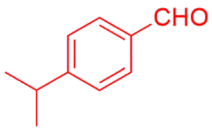	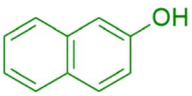	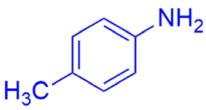	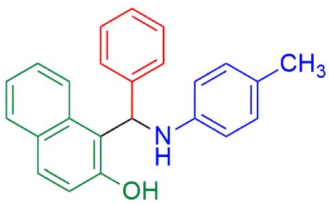	10	98
19	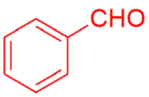	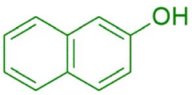	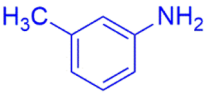	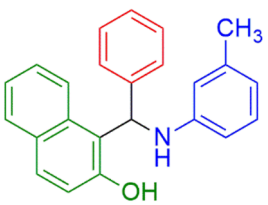	10	95
20	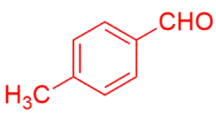	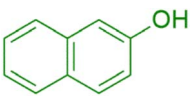	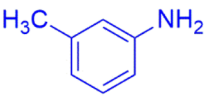	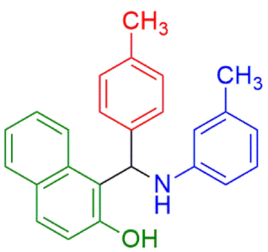	15	95

Table 2 (*Contd.*)

Sr. no.	Aldehyde (R)	Naphthol	Amide (R′)	Product	Time (min)	Yield[b] (%)
21	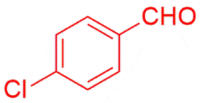	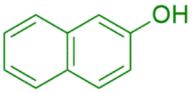	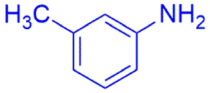	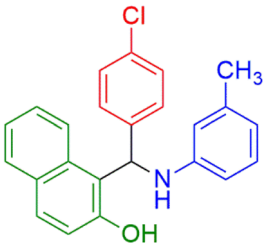	15	96

[a] Reaction conditions: reagents (10 mmol), nanocatalyst (0.08 mg) and β-naphthol (10 mmol) at 70 °C under solvent-free conditions. [b] Isolated yield.

2.2 Catalytic application of $Fe_3O_4@SiO_2@K_{10}$ nanoparticles in multicomponent reaction

Afterward, different analysis methods were used to analyze the generated nanoparticles, $Fe_3O_4@SiO_2@K_{10}$, it was investigated for its possible application in the manufacture of 1-amidoalkyl-2-naphthol analogs (Scheme 2). For this objective, the synthesis of amidoalkyl naphthol using β-naphthol, benzaldehyde, and benzamide was used as a model reaction to optimize the reaction conditions. During the investigation, it was revealed that the reaction of β-naphthol, benzaldehyde, and benzamide under solvent-free conditions, albeit at 90 °C, did not generate amidoalkyl naphthol. Notably, in the presence of 0.07 mg of $Fe_3O_4@SiO_2@K_{10}$ at the same temperature, the amido-alkyl naphthol reaction progressed successfully, yielding 85% after 40 minutes. Furthermore, lowering the temperature from 90 °C to 70 °C had no discernible effect on the reaction product. Unfortunately, lowering the temperature to 60 °C resulted in a reduction in the reaction product to 76%. Furthermore, increasing the nanoparticle quantity from 0.07 to 0.08 mg at 70 °C increased the reaction yield to 96%, however increasing the nanocatalyst amount to 0.09 mg had no impact on the entire productivity of the process. Several processes were carried out in polar aprotic (acetonitrile, THF), polar protic (methanol, ethanol), non-polar solvent (toluene), and mild polarity (DCM), but rates were unsatisfactory (Table 1).

The synthesis of amidoalkyl naphthol using several aromatic aldehydes, benzamide, and β-naphthol derivatives was carried out under these optimum conditions (Scheme 3). The presence of the electron-withdrawing substituent did not affect the yield of the aromatic aldehyde reaction when compared to the model reaction of aniline, according to the research (96% yield) (Table 2, Sr. no. 1–3). However, the derivatives with halogens (F, Cl, and Br) were slightly decreased yields as compared to the electron-withdrawing substrate (Table 2, Sr. no. 4–6). In the instance of benzaldehyde, however, the presence of an electron-donating group at the aromatic aldehyde resulted in a considerable fall in yield from 96% to 88% (Table 2, Sr. no. 7–10). Interestingly, aliphatic and heterocyclic aldehydes are more reactive than aromatic aldehydes (Table 2, Sr. no. 11–13). Then various aldehydes react with acetamide in the presence of β-naphthol derivatives containing the electron-withdrawing substrate giving better results (Table 2, Sr. no. 14–17). Finally, different aldehydes derivatives react with varieties of aromatic amines and β-naphthol giving the best result (Table 2, Sr. no. 18–21).

To study the recyclability of the prepared $Fe_3O_4@SiO_2@K_{10}$ nanocatalyst, for the synthesis of amidoalkyl naphthol using benzamide was taken as a model reaction. That after the reaction was completed, the nanoparticle was isolated from the reaction mass and employed even so during the next cycles. In addition, a hot filtration test was carried out during the production of amidoalkyl naphthol (Betti reaction) using benzamide, β-naphthol, and benzaldehyde to verify the heterogeneity of the $Fe_3O_4@SiO_2@K_{10}$ nanoparticle. After 25 minutes, the Betti reaction was performed to continue for another 25 minutes with the addition of $Fe_3O_4@SiO_2@K_{10}$ nanoparticle that had been separated from the mixture. No additional rise in the intended percentage yield was seen at the reaction's conclusion, indicating that the $Fe_3O_4@SiO_2@K_{10}$ nanoparticle is heterogeneous. The $Fe_3O_4@SiO_2@K_{10}$ nanocatalysthas been

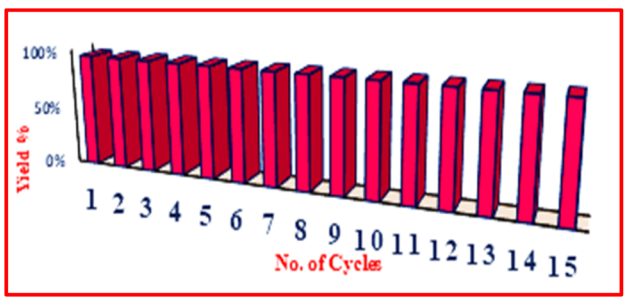

Fig. 8 Recyclability of the $Fe_3O_4@SiO_2@K_{10}$ nanocatalyst.

Table 3 Recoverable study of $Fe_3O_4@SiO_2@K_{10}$ nanocatalyst with percentage yield

Cycle	1	2	3	4	5	6	7	8	9	10	11	12	13	14	15
Yield (%)	96	96	96	96	96	95	95	95	95	94	94	94	93	93	93

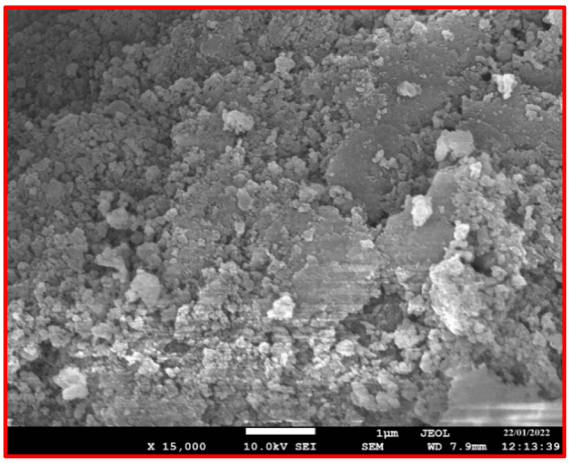

Fig. 9 SEM image of the Fe_3O_4@SiO_2@K_{10} nanocatalyst recycled after 15 times.

utilized for 15 cycles (Fig. 8) without losing its catalytic performance (Table 3).

Following the experiments for recyclability, the durability of the recovered Fe_3O_4@SiO_2@K_{10} nanoparticle was examined using SEM analysis. The SEM image showed that the recycled catalyst morphology is comparable to that of the initial catalyst. This finding demonstrated the excellent durability and retention of the Fe_3O_4@SiO_2@K_{10} nanoparticle structure (Fig. 9).

In aspects of the lowest rate of reaction, gentle condition, and harmful substances reduction, the current methodology is comparable to prior studies. The current nanocat-Fe-Si-K_{10} was significantly more effective than the previously reported work (Table 4). Additionally, after performing the reaction for a minimum of 15 cycles, the produced nanoparticle may be readily regenerated from the reaction medium without retaining its catalytic characteristics.

The possible mechanism (Scheme 4) confirmed up with previously reported work.[46] To create intermediate **I**, using MNPs first activates the aromatic aldehyde. The activating carbonyl substrate is then attacked by β-naphthol, yielding intermediate **II**. The *ortho*-quinone methides (*o*-QMs) intermediate **III** were then produced by eliminating H_2O from **II**. MNPs-SO_3H activation intermediate **III** once again, resulting in **IV** as a 1, 4 addition reaction. Following that, Michael adds benzamide to intermediate **IV**, resulting in the desired 1-amidoalkyl-2-naphthol. When comparison to aromatic aldehydes with electron-releasing groups, those with electron-withdrawing groups reacted rapidly.

3 Experimental section

The ESI† included all of the content and methodologies. As per the reported work, magnetic nanoparticles ferrite, silica ferrite, and K_{10} supported silica-coated ferrite were produced.

3.1 Synthesis Fe_3O_4@SiO_2@K_{10} nanoparticles[45,51]

While sonicating 1.2 g of Silica-coated ferrite nanoparticles in 100 mL of ethanol for around 30 minutes, then 0.53 g of montmorillonite (K_{10}) was added and mixed-phase during constant agitation. The pH of the working medium was then adjusted to 12 using a 1 M NaOH solution, and also the reaction mass was agitated for another 20 h at room temperature. Subsequently, the crystals were collected, rinsed with de-ionized water, and dried overnight at 60 °C to obtain 1.44 g of silica-coated magnetite-montmorillonite (K_{10}) nanoparticles.

3.2 Synthesis of amidoalkyl naphthol derivatives using nanocat-Fe-Si-K_{10}

A solvent-free reaction mass containing benzaldehyde (10 mmol), β-naphthol (10 mmol), benzamide (12 mmol), and Fe_3O_4@SiO_2@K_{10} (0.08 mg) were heated at 70 °C. Then the reaction progress was monitored using TLC (thin-layer chromatography). After the reaction was completed, the mixture was cooled to room temperature. Then, 5 mL ethyl acetate was added to the mixture, the catalyst was isolated using an external magnet, rinsed in alcohol, and dry at 60 °C for reusing. The ethyl acetate layer vaporized under lower pressure which got the pure product.

Table 4 Comparative study of preparation of amido-alkyl naphthol using nanocat-Fe-Si-K_{10} with some another catalyst reported in previous work

Sr. no.	Catalysts	Reaction condition	Yield (%)	Ref.
1	Trityl chloride	Room temperature, 4 h	94	32
2	Iodine	Solvent-free, 125 °C, 5 h	84	33
3	$Ce(SO_4)_2$	Acetonitrile, reflux, 36 h	78	34
4	$MgSO_4$	Solvent-free, 100 °C, 1 h	90	35
5	Imidazolium salt	Solvent-free, 120 °C, 40 min	95	36
6	$H_4SiW_{12}O_{40}$	Solvent-free, 110 °C	94	37
7	*p*-TSA	Solvent-free, 125 °C, 4–8 h	93	38
8	ZnO NPs	Solvent-free, (a) 130 °C, 30 min, (b) MW, 6 min	94	39
9	MNPs-HPZ-SO_3H	Solvent-free, 120 °C, 60 min	94	40
10	MNPs-Ph-SO_3H	Solvent-free, 120 °C, 40 min	94	41
11	Fe_3O_4@Mo NPs	Solvent-free, (a) 120 °C, 30 min, (b) MW. 3 min	94	42
12	Thiamine HCl (VB_1)	Ethanol, 80 °C, 4 h	78	43
13	Montmorillonite (K_{10})	Solvent-free, 125 °C, 1.5 h	78	44
14	Fe_3O_4@SiO_2@K_{10} NPs	Solvent-free, 70 °C, 25 min	96	Present work

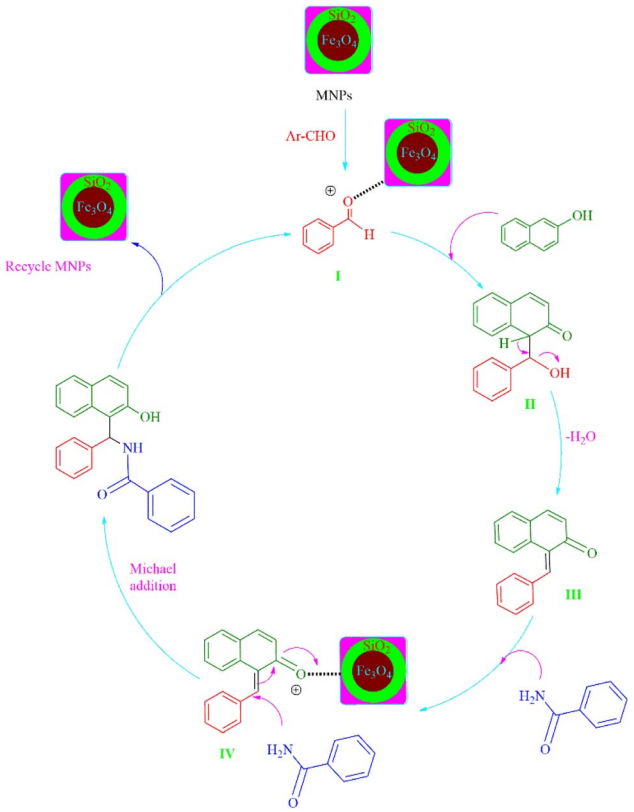

Scheme 4 Possible mechanistic path for synthesis of 1-amidoalkyl 2-naphthol.

4 Conclusion

In this study, we used K_{10} (montmorillonite) to coat on the surface of SiO_2@Fe_3O_4 nanoparticles, resulting in a silica-coating (Fe_3O_4@SiO_2@K_{10}) nanoparticles. The prepared nanoparticles have been useful for the production of 1-amidoalky-2-naphthol analogs. With regards to superior yield, shorter reaction times, low reaction temperature, recyclable catalyst, and a solvent-free system that promotes sustainable technology, this approach has numerous benefits over the previously reported work for the one-pot multicomponent synthesis of 1-amidoalkyl-2-naphthol derivatives. In addition, after 15 cycles, there was no substantial reduction of catalyst properties.

Conflicts of interest

There are no conflicts to declare.

Acknowledgements

The Chemistry Department, School of Chemical Engineering and Physical Science, Lovely Professional University, Phagwara-144411, Punjab, India, is acknowledged for its supporting work. Also grateful for the financial help provided by Principal of Dada Patil Mahavidyalaya, Karjat, for this research project (Seed Money Project).

Notes and references

1 H. Gao, J. Sun and C. Yan, *Chin. Chem. Lett.*, 2014, **26**, 353.
2 C. Cardellicchio, M. Capozzi and F. Naso, *Tetrahedron: Asymmetry*, 2010, **21**, 507.
3 A. Olyaei and M. Sadeghpour, *RSC Adv.*, 2019, **9**, 18467–18497.
4 A. Shen, C. Tsai and C. Chen, *Eur. J. Med. Chem.*, 1999, **34**, 877.
5 I. Szatmari, F. Fulop, I. Szatmári and F. Singh, *Curr. Org. Synth.*, 2004, **1**, 155.
6 H. Shaterian and H. Tandon, *Tetrahedron Lett.*, 2008, **49**, 1297.
7 A. Dewttignies, C. Len and A. Fihri, *ChemSusChem*, 2010, **5**, 502.
8 C. Mukhopadhyay, S. Rana and R. Butcher, *ARKIVOC*, 2010, **12**, 291.
9 I. Szatmari, A. Hetenyi, L. Lasar and F. Fulop, *J. Heterocycl. Chem.*, 2004, **41**, 567.
10 H. Gao, J. Sun and C. Yan, *Chin. Chem. Lett.*, 2015, **26**, 353.
11 T. Maegawa, Y. Kitamura, S. Sako, T. Udzu, A. Ai and A. Tanaka, *Chemistry*, 2007, **13**, 5937.
12 H. Moghanian, A. Mobinikhaledi, A. Blackman and E. Sorough-Farahani, *RSC Adv.*, 2014, **4**, 28176.
13 S. Kobayashi, H. Ishitani, S. Komiyama, D. Oniciu and A. Katritzky, *Tetrahedron Lett.*, 1996, **37**, 3731.
14 J. Mou, G. Gao, C. Chen, J. Liu, J. Gao, Y. Liu and D. Pei, *RSC Adv.*, 2017, **7**, 13868–13875.
15 B. Karmakar and J. Banerji, *Tetrahedron Lett.*, 2011, **52**, 4957.
16 A. Kumar, M. Gupta and M. Kumar, *Tetrahedron Lett.*, 2010, **51**, 1582.
17 A. Shahris, R. Teimuri-Mofrad and M. Gholamhosseini-Nazuri, *Mol. Diversity*, 2015, **19**, 1.
18 A. Rezaeifard, P. Farshid, M. Jafarpour and G. Moghaddam, *RSC Adv.*, 2014, **4**, 9189.
19 D. Seebac and J. Matthew, *Chem. Commun.*, 1997, **21**, 2015–2022.
20 Y. Wang, T. Izawa, S. Kobayashi and M. Ohno, *J. Am. Chem. Soc.*, 1982, **104**, 6465–6466.
21 S. Knapp, *Chem. Rev.*, 1995, **95**, 1859–1876.
22 A. Shen, C. Tsai and C. Chen, *Eur. J. Med. Chem.*, 1999, **34**, 877–882.
23 N. Selvam and P. Perumal, *Tetrahedron Lett.*, 2006, **47**, 7481–7483.
24 B. Das, K. Laxminarayana, B. Ravikanth and B. Rao, *J. Mol. Catal. A: Chem.*, 2007, **261**, 180–183.
25 L. Nagarapu, M. Baseeruddin, S. Apuri and S. Kantevari, *Catal. Commun.*, 2007, 1729–1734.
26 S. Kantevari, S. Vuppalapati and L. Nagarapu, *Catal. Commun.*, 2007, **8**, 1857–1862.
27 M. Zandi, A. Sardarian and C. R. Chimie, *RSC Adv.*, 2012, **15**, 365–369.
28 A. Supale and G. Gokavi, *J. Chem. Sci.*, 2010, **122**, 189–192.
29 H. Shaterian, A. Hosseinian and M. Ghashang, *Synth. Commun.*, 2008, **38**, 3766–3777.

30 H. Shaterian, H. Yarahmadi and M. Ghashang, *Bioorg. Med. Chem. Lett.*, 2008, **18**, 788–792.
31 M. Gawande and R. Jayaram, *Catal. Commun.*, 2006, **7**, 931.
32 A. Khazaei, M. Zolfigol, A. Zare, A. Parhami and A. Nezhad, *Appl. Catal., A*, 2010, **386**, 179.
33 Q. Zhang, J. Luo and Y. Wei, *Green Chem.*, 2010, **12**, 2246.
34 N. Selvam and P. Perumal, *Tetrahedron Lett.*, 2006, **47**, 7481.
35 K. Ashalu and J. Rao, *J. Chem. Pharm. Res.*, 2013, **5**, 44–47.
36 M. Zolfigol, A. Khazaei, A. Zare and V. Khakyzadeh, *Appl. Catal., A*, 2011, **400**, 70.
37 A. Supale and G. Gokavi, *J. Chem. Sci.*, 2010, **122**, 189.
38 M. Khodaei, A. Khosropour and H. Moghanian, *Synlett*, 2016, **6**, 916.
39 R. Singh, R. Bala and S. Kumar, *Indian J. Chem., Sect. B: Org. Chem. Incl. Med. Chem.*, 2016, **55**, 381.
40 Z. Nasresfahani, M. Kassaee and E. Eidi, *New J. Chem.*, 2016, **40**, 4720.
41 H. Moghanian, A. Mobinikhaledi and A. Blackman, *RSC Adv.*, 2014, **4**, 28176.
42 S. Bankar and S. Shelke, *Res. Chem. Intermed.*, 2017, **44**, 3507–3521.
43 M. Lei, *Tetrahedron Lett.*, 2009, **50**, 6393–6397.
44 S. Kantevari and L. Nagarapu, *Catal. Commun.*, 2007, **8**, 1857.
45 N. Tandon, S. Patil, R. Tandon and P. Kumar, *RSC Adv.*, 2021, **11**, 21291–21300.
46 J. Safari and Z. Zarnegar, *J. Mol. Catal. A: Chem.*, 2013, **379**, 269–276.
47 S. Patil, R. Tandon and N. Tandon, *Curr. Res. Green Sustainable Chem.*, 2021, **4**, 100063.
48 R. Tandon, S. Patil, N. Tandon and P. Kumar, *Lett. Org. Chem.*, 2022, **19**, 1570.
49 A. Ingale, S. Patil and S. Shinde, *Tetrahedron Lett.*, 2017, **58**, 52.
50 R. Tandon, N. Tandon and S. Patil, *RSC Adv.*, 2021, **11**, 29333–29353.
51 S. Patil, R. Tandon and N. Tandon, *J. Phys.: Conf. Ser.*, 2022, **2267**, 012107.
52 S. Patil, *Int. J. Pharm. Res.*, 2017, **13**, 317.
53 S. Patil, R. Tandon and N. Tandon, *ACS Omega*, 2022, **28**, 24190–24201.
54 S. Patil, A. Ingale, A. Pise and R. Bhondave, *ChemistrySelect*, 2022, **7**, 1–9.
55 S. Patil, R. Tandon and N. Tandon, *Pharm. Pat. Anal.*, 2022, **11**, 175–186.